

---

---

# Brown Fat Imaging with $^{18}\text{F}$ -6-Fluorodopamine PET/CT, $^{18}\text{F}$ -FDG PET/CT, and $^{123}\text{I}$ -MIBG SPECT: A Study of Patients Being Evaluated for Pheochromocytoma

Mohiuddin Hadi<sup>1</sup>, Clara C. Chen<sup>1</sup>, Millie Whatley<sup>1</sup>, Karel Pacak<sup>2</sup>, and Jorge A. Carrasquillo<sup>1</sup>

<sup>1</sup>Department of Nuclear Medicine, Warren Grant Magnuson Clinical Center, National Institutes of Health, Bethesda, Maryland; and

<sup>2</sup>Pediatric and Reproductive Endocrinology Branch, National Institute of Child Health and Human Development, National Institutes of Health, Bethesda, Maryland

---

Several radiopharmaceuticals such as  $^{18}\text{F}$ -FDG,  $^{123}\text{I}$ -metaiodobenzylguanidine (MIBG), and  $^{99\text{m}}\text{Tc}$ -tetrofosmin have demonstrated uptake in brown adipose tissue (BAT). It is important to recognize these normal variants so that they are not misinterpreted as a significant pathologic state. In addition, these radiopharmaceuticals may shed light on BAT physiology.  $^{18}\text{F}$ -6-fluorodopamine (F-DA) is being used as a PET radiopharmaceutical to image adrenergic innervation and suspected pheochromocytoma. Past reports have suggested that BAT is increased in pheochromocytoma patients. **Methods:** The images of 96 patients evaluated with  $^{18}\text{F}$ -F-DA or  $^{18}\text{F}$ -FDG PET/CT for known or suspected pheochromocytoma were reviewed retrospectively to determine whether localized uptake of a pattern typically associated with BAT was present. When available, contemporaneous images obtained using  $^{123}\text{I}$ -MIBG were also reviewed for the presence of BAT. **Results:** Of 67 patients imaged with  $^{18}\text{F}$ -F-DA, BAT was found in 17.9%. Of 83 patients imaged with  $^{18}\text{F}$ -FDG, 19.2% had BAT. Discordant findings related to uptake in BAT were often seen in patients studied with  $^{18}\text{F}$ -FDG,  $^{18}\text{F}$ -F-DA, or  $^{123}\text{I}$ -MIBG. Overall, 26 (27.0%) of 96 patients showed BAT on at least 1 of the 3 imaging modalities. **Conclusion:**  $^{18}\text{F}$ -F-DA can image BAT, most likely by localizing to sympathetic innervations in a manner similar to  $^{123}\text{I}$ -MIBG. Patients with pheochromocytoma may have a greater BAT tissue mass or activation because of elevated levels of circulating catecholamines. Quantitative PET with  $^{18}\text{F}$ -FDG and  $^{18}\text{F}$ -F-DA may have a role in in vivo studies of BAT physiology in humans or animal models.

**Key Words:** PET; PET/CT; brown fat;  $^{18}\text{F}$ -FDG;  $^{123}\text{I}$ -MIBG;  $^{18}\text{F}$ -fluorodopamine

**J Nucl Med 2007; 48:1077–1083**

DOI: 10.2967/jnumed.106.035915

---

A variety of radiopharmaceuticals used in nuclear medicine, such as  $^{18}\text{F}$ -FDG,  $^{99\text{m}}\text{Tc}$ -tetrofosmin, and  $^{123}\text{I}$ -metaiodobenzylguanidine (MIBG), have been reported to localize in brown adipose tissue (BAT) (1–7). It is important for the physician interpreting these images to recognize these patterns so as not to confuse them with a pathologic state. Furthermore, identifying which radiopharmaceuticals localize in BAT may give insights as to their mechanism of localization and BAT physiology. BAT has an abundant supply of sympathetic nerves that are important in its physiology and that may be amenable to imaging with  $^{18}\text{F}$ -6-fluorodopamine (F-DA), and various studies have documented increased glucose metabolism in BAT (8). The study of BAT has attracted interest in the field of obesity (9–13) and glucose homeostasis (14). Thus, radiopharmaceuticals that can assess pathways important in BAT physiology may be useful.

It has been suggested that the incidence of BAT may be higher in patients with pheochromocytoma than in patients without (15–18). After identifying an index patient studied with  $^{18}\text{F}$ -F-DA who had a neck and supraclavicular activity distribution similar to that described for  $^{18}\text{F}$ -FDG as typical of BAT, we searched for similar  $^{18}\text{F}$ -F-DA,  $^{18}\text{F}$ -FDG, or  $^{123}\text{I}$ -MIBG uptake in a group of patients we had previously evaluated for pheochromocytoma. To our knowledge, this report is the first of uptake in BAT of  $^{18}\text{F}$ -F-DA, which is a radiopharmaceutical that has been used to image sympathetic innervations (19) and localize pheochromocytomas (20).

## MATERIALS AND METHODS

This study was a retrospective review evaluating the presence of BAT in patients undergoing  $^{18}\text{F}$ -F-DA PET/CT imaging.  $^{18}\text{F}$ -F-DA was used under an investigational new drug application approved by the Food and Drug Administration. Patients were evaluated for suspected or proven pheochromocytoma in a protocol approved by the National Institute of Child Health and Human Development Institutional Review Board. All patients gave written informed consent for  $^{18}\text{F}$ -F-DA scans. When these patients also

---

Received Oct. 28, 2006; revision accepted Apr. 3, 2007.

For correspondence contact: Jorge A. Carrasquillo, MD, 1275 York Ave., New York, NY 10021.

E-mail: carrasj1@mskcc.org

COPYRIGHT © 2007 by the Society of Nuclear Medicine, Inc.

underwent  $^{18}\text{F}$ -FDG PET/CT or  $^{123}\text{I}$ -MIBG for clinical indications, the contemporaneous studies were also evaluated for the presence of BAT. Contemporaneous imaging studies were defined as those performed within 30 d of each other, without major intervening therapy or surgery.

We reviewed the studies of 96 patients (39 male and 57 female) who were referred for evaluation of suspected or proven pheochromocytoma. These patients underwent  $^{18}\text{F}$ -F-DA PET/CT or  $^{18}\text{F}$ -FDG PET/CT between February 2004 and May 2006 at the National Institutes of Health (NIH) Clinical Center. Their mean age was 46.6 y (range, 13–89 y). Only 2 patients were less than 18 y old. In these 96 patients, we reviewed a total of 84  $^{18}\text{F}$ -F-DA PET/CT studies, 93  $^{18}\text{F}$ -FDG PET/CT studies, and 62  $^{123}\text{I}$ -MIBG studies that were contemporaneous with either of the PET/CT studies. All 62  $^{123}\text{I}$ -MIBG studies were contemporaneous with an  $^{18}\text{F}$ -FDG PET/CT study, and in 34 patients, the  $^{18}\text{F}$ -FDG and  $^{18}\text{F}$ -F-DA PET/CT studies were contemporaneous. Twenty-four patients had a  $^{123}\text{I}$ -MIBG study contemporaneous with the  $^{18}\text{F}$ -F-DA study, and in 23 patients, all 3 studies were contemporaneous.

### Scanning Protocols

$^{18}\text{F}$ -F-DA and  $^{18}\text{F}$ -FDG PET/CT were performed using a Discovery LS PET/CT camera (GE Healthcare) after a fast of at least 6 h (typically overnight), with approximately 37 MBq (1 mCi) of  $^{18}\text{F}$ -F-DA and 555 MBq (15 mCi) of  $^{18}\text{F}$ -FDG injected intravenously. Imaging from the skull to the proximal thigh was performed starting 10 min after radiopharmaceutical injection for  $^{18}\text{F}$ -F-DA and 1 h after injection for  $^{18}\text{F}$ -FDG. For  $^{123}\text{I}$ -MIBG, planar whole-body imaging and SPECT were performed at 24 h for all patients and at 48 h for selected patients after injection of about 370 MBq (10 mCi) of  $^{123}\text{I}$ -MIBG, on either a dual-head e-Cam  $\gamma$ -camera (Siemens Medical Systems), a triple-head Triad XLT  $\gamma$ -camera (Trionix Inc.), or a dual-head Vertex  $\gamma$ -camera (Philips) using a low-energy all-purpose collimator. All patients received a saturated solution of potassium iodide for thyroid blockade before  $^{123}\text{I}$ -MIBG injection.

### Image Processing and Review

All PET data was acquired in 2-dimensional mode and reconstructed iteratively using the manufacturers' software. CT was used for attenuation correction.  $^{123}\text{I}$ -MIBG SPECT studies were reconstructed using filtered backprojection. All  $^{123}\text{I}$ -MIBG and PET datasets were reviewed in 3 orthogonal views and as

rotating maximum-intensity-projection data using a MedView workstation (MedImage). Two nuclear medicine physicians reported the presence or absence of BAT in the nuchal, supraclavicular, and paravertebral regions, using the CT scan to confirm localization to adipose tissue. For  $^{123}\text{I}$ -MIBG studies lacking CT for coregistration, the presence of BAT was inferred from the characteristic distribution pattern. Discordance was resolved by consensus. When, occasionally, a consensus could not be achieved, a third nuclear medicine physician was consulted to resolve the findings. All readers reviewed the images of a given modality independently of the other 2 modalities and unaware of plasma catecholamine levels and final diagnosis.

The voxel values of the  $^{18}\text{F}$ -F-DA and  $^{18}\text{F}$ -FDG images were converted to standardized uptake values (SUVs) corrected for lean body mass (21), as follows:  $\text{SUV} = \text{voxel activity (in Bq/mL)} / [\text{injected dose (in Bq)/gram of lean body mass}]$ .

When BAT was identified, maximum SUVs were obtained from regions of interest manually drawn on representative areas of BAT uptake, because SUVs provide some quantitative measure of the radiopharmaceutical uptake and facilitate comparison with previous  $^{18}\text{F}$ -FDG reports.

### BAT Findings on $^{18}\text{F}$ -F-DA and $^{18}\text{F}$ -FDG PET/CT

To determine how frequently BAT was observed on  $^{18}\text{F}$ -F-DA or  $^{18}\text{F}$ -FDG PET/CT, we included only the first study of each type in the analysis when multiple instances of the study were performed on a single patient. The initial study was used, rather than all instances, because the initial studies would be independent of each other and thus would not bias the data through inclusion of multiple follow-up studies of the same patient.

### Comparison of BAT Findings in Contemporaneous Studies Using $^{18}\text{F}$ -F-DA, $^{18}\text{F}$ -FDG, and $^{123}\text{I}$ -MIBG

In several cases, 2 or 3 modalities (i.e.,  $^{18}\text{F}$ -F-DA PET/CT and  $^{18}\text{F}$ -FDG PET/CT,  $^{18}\text{F}$ -FDG PET/CT and  $^{123}\text{I}$ -MIBG,  $^{18}\text{F}$ -F-DA PET/CT and  $^{123}\text{I}$ -MIBG, or all 3 modalities) were performed contemporaneously, without major intervening therapy or surgery. We studied the concordance of BAT findings in these studies between  $^{18}\text{F}$ -F-DA and contemporaneous  $^{123}\text{I}$ -MIBG, between  $^{18}\text{F}$ -F-DA and contemporaneous  $^{18}\text{F}$ -FDG, and between all 3 modalities when contemporaneous.

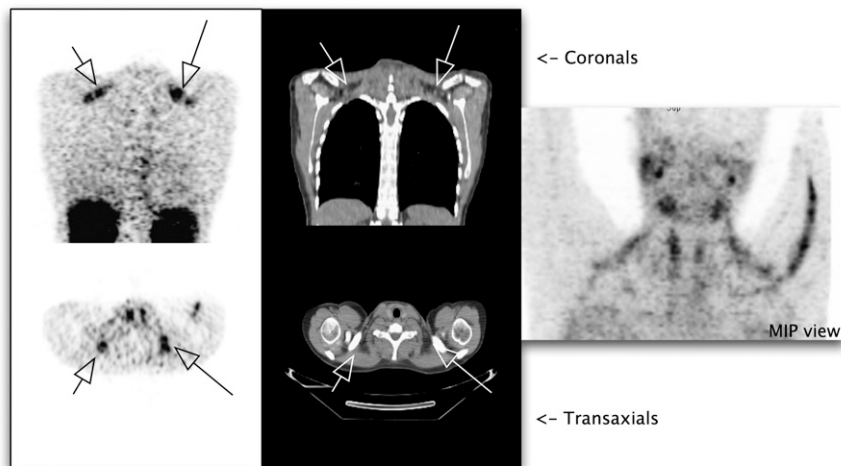


**FIGURE 1.** Patient 10 with pheochromocytoma showing  $^{18}\text{F}$ -F-DA uptake in supraclavicular BAT (black arrows) that corresponded to fat on coregistered CT (white arrows). At far right is maximum-intensity-projection image showing some uptake typical of  $^{18}\text{F}$ -F-DA (salivary gland, thyroid, vein in left upper extremity) and uptake in supraclavicular areas corresponding to BAT.

### Comparison of Plasma Norepinephrine and Epinephrine Values with BAT Findings

Because circulating catecholamine levels may reflect sympathetic nervous activity with the possibility of stimulating BAT directly and/or interfering with  $^{18}\text{F}$ -F-DA binding, we compared BAT visualization to catecholamine levels. Contemporaneous plasma norepinephrine and epinephrine measurements performed within 3 d

before or after either PET/CT study were obtained when available, and the median values were compared in patients with and without visualization of BAT. The differences between distributions of catecholamine levels in these groups were assessed for significance using the Mann–Whitney *U* test. The proportions of BAT positivity in patients with normal or elevated catecholamine levels were assessed for significance using the Fisher exact test.

**TABLE 1**  
Patients with BAT Visualization on One or More Studies

Patient no.	Age (y)	Sex	SUV*			Final diagnosis	Associated PET/CT study†	
			$^{18}\text{F}$ -FDG PET/CT	$^{18}\text{F}$ -F-DA PET/CT	$^{123}\text{I}$ -MIBG SPECT		Plasma norepinephrine (pg/mL)	Plasma epinephrine (pg/mL)
1	48	F	N	NA	P	Pheo	1,712, $^{18}\text{F}$ -F-DA	
2	17	M	NA	P (4.3)	NA	Not pheo	351, $^{18}\text{F}$ -F-DA	72, $^{18}\text{F}$ -F-DA
3	40	M	P (3.8)	NA	NA	Pheo	2,791, $^{18}\text{F}$ -FDG	24, $^{18}\text{F}$ -FDG
4	25	F	P (2.4)	N	NA	Pheo	2,791, $^{18}\text{F}$ -F-DA	24, $^{18}\text{F}$ -F-DA
5	32	F	N	NA	P	Pheo	2,569, $^{18}\text{F}$ -F-DA	
6	56	F	N	N	P	Not pheo	NA	NA
7	39	F	P (4.1)	N	N	Pheo	400, $^{18}\text{F}$ -FDG	18, $^{18}\text{F}$ -FDG
8	29	M	P (1.4)	N	P	Pheo	400, $^{18}\text{F}$ -F-DA	18, $^{18}\text{F}$ -F-DA
9	26	F	P (9.0)	NA	N	Pheo	767, $^{18}\text{F}$ -F-DA	NA
10	27	F	NA	P (3.4)	NA	Pheo	27,456, $^{18}\text{F}$ -FDG	15, $^{18}\text{F}$ -FDG
11	38	F	P (1.6)	NA	NA	Pheo	27,456, $^{18}\text{F}$ -F-DA	15, $^{18}\text{F}$ -F-DA
12	38	F	N	P (2.1)	NA	Not pheo	141,299, $^{18}\text{F}$ -FDG	129, $^{18}\text{F}$ -FDG
13	49	F	P (2.0)	NA	NA	Not pheo	496, $^{18}\text{F}$ -F-DA	7, $^{18}\text{F}$ -F-DA
14	34	M	N	P (4.4)	N	Pheo	1,510, $^{18}\text{F}$ -F-DA	40, $^{18}\text{F}$ -F-DA
15a‡	30	M	P (3.2)	P (1.5)	N	Pheo	225, $^{18}\text{F}$ -FDG	34, $^{18}\text{F}$ -FDG
15b‡	29	M	P (17.7)	NA	NA	Pheo	225, $^{18}\text{F}$ -F-DA	34, $^{18}\text{F}$ -F-DA
16§	29	M	N§	P (3.0)§	P§	Pheo	1,301, $^{18}\text{F}$ -FDG	16, $^{18}\text{F}$ -FDG
17a‡	26	F	NA	P (3.6)	NA	Previous pheo	549, $^{18}\text{F}$ -FDG	59, $^{18}\text{F}$ -FDG
17b‡	26	F	P (5.0)	NA	P	Previous pheo	549, $^{18}\text{F}$ -F-DA	59, $^{18}\text{F}$ -F-DA
18	24	F	P (8.0)	P (2.0)	NA	Pheo	31,429, $^{18}\text{F}$ -F-DA	86, $^{18}\text{F}$ -F-DA
19	66	F	P (1.6)	NA	NA	Pheo	NA	NA
20	33	M	P (5.4)	NA	P	Pheo	261, $^{18}\text{F}$ -F-DA	38, $^{18}\text{F}$ -F-DA
21	17	F	N	P (2.0)	P	Not pheo	210, $^{18}\text{F}$ -F-DA	18, $^{18}\text{F}$ -F-DA
22	38	F	P (3.5)	NA	P	Not pheo	278, $^{18}\text{F}$ -FDG	7, $^{18}\text{F}$ -FDG
23a‡	28	M	P (5.0)	NA	P	Pheo	598, $^{18}\text{F}$ -F-DA	4, $^{18}\text{F}$ -F-DA
23b‡	28	M		P (1.8)	NA	Pheo	22,587, $^{18}\text{F}$ -FDG	64, $^{18}\text{F}$ -FDG
24	13	M	P (4.6)	P (4.8)	P	Pheo	895, $^{18}\text{F}$ -F-DA	NA
25	19	F	N	P (2.0)	N	Neuroblastoma	1,093, $^{18}\text{F}$ -FDG	26, $^{18}\text{F}$ -FDG
26	22	M	P (1.0)	N	N	Pheo	1,093, $^{18}\text{F}$ -F-DA	26, $^{18}\text{F}$ -F-DA
Positive findings			17 (16)	12	11		349, $^{18}\text{F}$ -FDG	19, $^{18}\text{F}$ -FDG
							NA	NA
							NA	NA
							3,407, $^{18}\text{F}$ -F-DA	10, $^{18}\text{F}$ -F-DA
							888, $^{18}\text{F}$ -FDG	NA
							888, $^{18}\text{F}$ -F-DA	
							1,811, $^{18}\text{F}$ -FDG	3, $^{18}\text{F}$ -FDG
							1,811, $^{18}\text{F}$ -F-DA	3, $^{18}\text{F}$ -F-DA

\*SUV is reported only for BAT+. Findings: P = positive for BAT; N = negative for BAT; NA = data not available.

†Plasma catecholamine was measured within 0–3 d of corresponding PET/CT study. In some cases, both PET/CT studies were within 3 d of laboratory measurement.

‡Same patient with 1 positive result on different modalities several months apart (on different modalities or contemporaneous with different modalities).

§Chronologic order of studies in this patient was first  $^{18}\text{F}$ -F-DA, then  $^{123}\text{I}$ -MIBG, and finally  $^{18}\text{F}$ -FDG.  $^{18}\text{F}$ -FDG study was not contemporaneous (41 d) with  $^{18}\text{F}$ -F-DA but was contemporaneous with  $^{123}\text{I}$ -MIBG;  $^{18}\text{F}$ -F-DA and  $^{123}\text{I}$ -MIBG studies were contemporaneous.

Pheo = pheochromocytoma.

### Comparison with Final Diagnosis

Pheochromocytoma was confirmed in 65 patients on histopathologic examination. Three patients had prior pheochromocytoma and were in remission, and 1 patient could not be followed up. The remaining patients were classified as not having pheochromocytoma. BAT visualization on the 3 imaging modalities was compared with the final diagnosis and statistically assessed for significance using the Fisher exact test.

## RESULTS

### Detection of BAT

Review of the  $^{18}\text{F}$ -F-DA PET/CT studies performed on 67 patients revealed BAT in 12 studies (17.9%), with a representative study shown in Figure 1. Review of the  $^{18}\text{F}$ -FDG PET/CT studies performed on 83 patients revealed the presence of BAT in 16 (19.3%). Eleven (17.7%) of the 62  $^{123}\text{I}$ -MIBG studies demonstrated BAT. BAT was visualized on at least 1 of the 3 modalities in 26 patients (27.1%) of the total of 96 (Table 1).

### Comparison of $^{18}\text{F}$ -F-DA Findings with $^{18}\text{F}$ -FDG and $^{123}\text{I}$ -MIBG

Thirty-four patients underwent contemporaneous  $^{18}\text{F}$ -F-DA and  $^{18}\text{F}$ -FDG PET/CT. The presence or absence of BAT findings on these studies is depicted in Table 2. Twenty-four patients underwent contemporaneous  $^{18}\text{F}$ -F-DA PET/CT and  $^{123}\text{I}$ -MIBG; the results are shown in Table 3. Only 23 patients were contemporaneously imaged with all 3 modalities, as shown in Table 4. Of these patients, 11 were concordantly negative for BAT across all 3 modalities, whereas 6, 4, and 2 patients were positive for BAT on 1, 2, or all 3 studies, respectively. Figure 2 shows an example of BAT visualized on all 3 studies.

### Relationship of Plasma Norepinephrine and Epinephrine Levels to $^{18}\text{F}$ -F-DA and $^{18}\text{F}$ -FDG

Table 5 summarizes the relationship of plasma norepinephrine and epinephrine levels to  $^{18}\text{F}$ -F-DA and  $^{18}\text{F}$ -FDG. Of patients who were BAT-positive on  $^{18}\text{F}$ -FDG, 75% (6/8) had elevated plasma norepinephrine levels, whereas 47% (15/32) who were BAT-negative on  $^{18}\text{F}$ -FDG also had elevated norepinephrine levels. However, for  $^{18}\text{F}$ -FDG, the median norepinephrine level was significantly higher in BAT-positive patients ( $P = 0.01$ ). In contrast, 45% (5/11) of patients with BAT-positive and 72% (34/47) of those with BAT-negative  $^{18}\text{F}$ -F-DA scans had elevated plasma norepinephrine levels. In addition, the median plasma norepinephrine levels in the 2 groups, although elevated in both, was lower in patients who

**TABLE 2**  
BAT Findings on  $^{18}\text{F}$ -F-DA and  $^{18}\text{F}$ -FDG Scans

$^{18}\text{F}$ -F-DA PET/CT	$^{18}\text{F}$ -FDG PET/CT		No. of patients
	BAT+	BAT-	
BAT+	3	4	7
BAT-	6	21	27
	9	25	34

**TABLE 3**  
BAT Findings on  $^{18}\text{F}$ -F-DA and  $^{123}\text{I}$ -MIBG Scans

$^{18}\text{F}$ -F-DA PET/CT	$^{123}\text{I}$ -MIBG		No. of patients
	BAT+	BAT-	
BAT+	4	3	7
BAT-	3	14	17
	7	17	24

were BAT-positive on  $^{18}\text{F}$ -F-DA studies than in BAT-negative patients. These relationships were found to be statistically nonsignificant.

Irrespective of BAT findings in either PET study, median plasma epinephrine levels were within normal limits in all groups.

### Comparison of BAT Visualization with Final Diagnosis

BAT visualization in the 65 patients who had pheochromocytoma at the time of imaging, and in 27 patients who never had pheochromocytoma, are summarized in Table 6 for each modality. The proportions were not significantly different for any modality.

## DISCUSSION

BAT is a morphologically and functionally distinct component of the adipose organ in mammals. Histologically, BAT is characterized by small cells, multilocularity, large numbers of mitochondria, increased vascularity, and abundant sympathetic noradrenergic innervations, compared with the more widespread white adipose tissue. Norepinephrine is a key regulator of BAT that stimulates lipolysis, glucose transport, and uncoupling protein-1 expression in brown adipocytes, as well as an increase in BAT adipocyte numbers (8). The amount and distribution of BAT vary with age, nutrition, and environment (22). Thus, a radiopharmaceutical that evaluates adrenergic pathways may be of use in understanding BAT physiology.

Uptake of  $^{18}\text{F}$ -FDG in BAT has been well recognized (2,3,23).  $^{18}\text{F}$ -FDG localization in BAT can be attributed to

**TABLE 4**  
BAT Findings for Patients with 3 Contemporaneous Imaging Studies

Finding	$^{18}\text{F}$ -FDG	$^{18}\text{F}$ -F-DA	$^{123}\text{I}$ -MIBG	No. of patients
All negative	N	N	N	11
One positive	P	N	N	3
	N	P	N	2
	N	N	P	1
Two positive	P	P	N	1
	N	P	P	1
	P	N	P	2
All positive	P	P	P	2
Total				23

N = negative for BAT; P = positive for BAT.

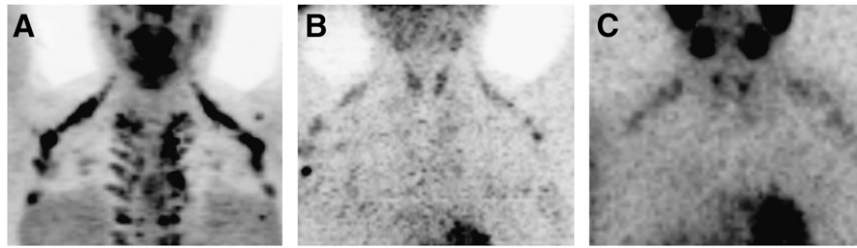


**FIGURE 2.** Maximum-intensity-projection images of patient 18 with pheochromocytoma.  $^{18}\text{F}$ -FDG PET (A) shows typical BAT uptake in supraclavicular region extending into axilla and paravertebral regions.  $^{18}\text{F}$ -F-DA PET (B) and  $^{123}\text{I}$ -MIBG SPECT (C) show BAT uptake in supraclavicular regions. Uptake in paraspinal regions is best seen on  $^{18}\text{F}$ -FDG images.

noradrenergic stimulation through  $\beta_3$  receptors, resulting in increased expression of uncoupling protein-1 and increased glucose uptake. Uncoupling protein-1 is the uncoupling protein that bypasses proton-flux-driven adenosine triphosphate synthesis in the mitochondria and thereby results in thermogenesis (8). Several imaging studies have suggested the importance of sympathetic innervation in imaging of BAT with  $^{123}\text{I}$ -MIBG (16,24–26). Two reports have described  $^{18}\text{F}$ -FDG or  $^{123}\text{I}$ -MIBG imaging of BAT in patients with extraadrenal pheochromocytoma (27,28). In both cases, repeated imaging studies after surgical resection of pheochromocytoma showed that BAT had disappeared, suggesting that perhaps the lack of uptake on follow-up was due to resolution of the sympathetic stimuli. We postulate that the mechanism of uptake of  $^{18}\text{F}$ -F-DA seen in BAT may be

similar to that of  $^{123}\text{I}$ -MIBG, given that  $^{18}\text{F}$ -F-DA and  $^{123}\text{I}$ -MIBG have similar mechanisms of uptake (19,29–31).

The incidence of accumulation in BAT in most  $^{18}\text{F}$ -FDG PET/CT studies has ranged from 2.3% to 6.7% (1,3,4,23), with a single  $^{18}\text{F}$ -FDG PET series showing an incidence of 31% of “neck and upper chest uptake” without coregistered CT (32). For  $^{123}\text{I}$ -MIBG, the percentage of patients with BAT visualization was reported to be 12% by Okuyama et al. in a pediatric population with neuroendocrine tumors (7). The overall incidence of BAT visualization was higher in our study than in most of the series reported to date: 19.2% with  $^{18}\text{F}$ -FDG, 17.9% with  $^{18}\text{F}$ -F-DA, and 17.7% with  $^{123}\text{I}$ -MIBG. Although this higher incidence may be related, in part, to our close scrutiny of the images and awareness of the BAT pattern, the  $^{18}\text{F}$ -FDG SUVs in our patients were in the range of

**TABLE 5**  
Comparison of Plasma Catecholamine Levels with BAT Findings on PET/CT

Level	BAT+	BAT–	<i>n</i>	<i>P</i>
$^{18}\text{F}$ -F-DA				
Elevated norepinephrine (>498 pg/mL)	5	34	58	0.18*
Normal norepinephrine	6	13		
Plasma norepinephrine (pg/mL)				
Mean $\pm$ SD	3,591 $\pm$ 9,277	1,878 $\pm$ 4,111		0.38†
Median	549	885		
Elevated epinephrine (>83 pg/mL)	1	5	45	1.00*
Normal epinephrine	9	30		
Plasma epinephrine (pg/mL)				
Mean $\pm$ SD	35 $\pm$ 28	48.9 $\pm$ 103		0.66†
Median	30	18		
$^{18}\text{F}$ -FDG				
Elevated norepinephrine (>498 pg/mL)	6	15	40	0.30*
Normal norepinephrine	2	17		
Norepinephrine (pg/mL)				
Mean $\pm$ SD	24,734 $\pm$ 48,326	1,391 $\pm$ 3,088		0.01†
Median	2,301	419		
Elevated epinephrine (>83 pg/mL)	1	5	35	1.00*
Normal epinephrine	6	23		
Plasma epinephrine (pg/mL)				
Mean $\pm$ SD	34 $\pm$ 42	133 $\pm$ 481		0.39†
Median	17.5	22		

\*Fisher exact test.

†Mann-Whitney *U* test.

**TABLE 6**  
BAT Visualization in All Patients, Classified by Imaging Modality and Final Diagnosis

Modality	Pheochromocytoma ( <i>n</i> = 65)	Not pheochromocytoma* ( <i>n</i> = 27)	All patients† ( <i>n</i> = 96)
<sup>18</sup> F-F-DA+	7/48 (14.6%)	4/15 (26.6%)	12/67 (17.9%)
<sup>18</sup> F-F-DA-	41/48 (85.4%)	11/15 (73.4%)	55/67 (82.1%)
<sup>18</sup> F-FDG+	13/59 (22%)	2/21 (9.5%)	16/83 (19.3%)
<sup>18</sup> F-FDG-	46/59 (78%)	19/21 (90.5%)	67/83 (80.7%)
<sup>123</sup> I-MIBG+	7/45 (15.5%)	3/16 (18.8%)	11/62 (17.7%)
<sup>123</sup> I-MIBG-	38/45 (84.5%)	13/16 (81.2%)	51/62 (82.3%)

\*Excluding 3 patients in remission and 1 lost to follow-up.

†Including 3 patients in remission and 1 lost to follow-up.

those reported by Yeung et al. (4), particularly when one considers that our SUVs were corrected for lean body mass rather than body weight, which generally results in lower values for lean body mass. More likely, some of the differences in incidence were due to our patient population, namely patients with diagnosed or suspected pheochromocytoma. Patients with pheochromocytoma have been postulated by others to have an increased incidence of BAT, presumably because of the high circulating norepinephrine levels (15–18).

Although we saw <sup>18</sup>F-FDG uptake in BAT in a higher proportion of patients with confirmed pheochromocytoma than of patients who were subsequently found not to have pheochromocytoma, this difference was not statistically significant. Interestingly, elevated catecholamines were found in a higher proportion of patients showing BAT on <sup>18</sup>F-FDG than in BAT-negative patients, and the median catecholamine levels were significantly higher in the former group. These findings are consistent with prior reports indicating that norepinephrine activates glucose transport (33,34).

In contrast to <sup>18</sup>F-FDG, <sup>18</sup>F-F-DA revealed BAT in a higher proportion of patients without pheochromocytoma than of those with pheochromocytoma. Similarly, a higher proportion of patients without than with <sup>18</sup>F-F-DA uptake in BAT had elevated norepinephrine levels, and the median norepinephrine levels were higher in the former group. Because the difference between norepinephrine levels in these 2 groups was not statistically significant, we cannot exclude that this reversal occurred by chance alone. That stated, a possible explanation could be that the elevated plasma norepinephrine levels may have competed with <sup>18</sup>F-F-DA for norepinephrine transporter, thus reducing the uptake of <sup>18</sup>F-F-DA in BAT. A similar inverse relationship has been found with respect to cardiac uptake of <sup>18</sup>F-F-DA and <sup>123</sup>I-MIBG in the presence of elevated catecholamines (35,36). Also, although pheochromocytoma was excluded in 27 patients, these patients were not necessarily healthy, many having been referred because of signs or symptoms that led to a suspicion of pheochromocytoma. Thus, although we did not see statistically significant differences in BAT visualization using <sup>18</sup>F-FDG, <sup>18</sup>F-F-DA, or <sup>123</sup>I-MIBG between patients with and without pheochromocytoma, we cannot conclude

that such a difference does not exist. Comparison with a group of healthy, asymptomatic subjects would be instructive.

As seen in Tables 3 and 4, visualization of BAT with different radiopharmaceuticals was often incongruent. Several factors may have contributed to this finding. Because this study was retrospective, we did not monitor or control room temperature (37) or medication use, variations in either of which could have caused real physiologic differences in BAT status.

The study of BAT has attracted interest related to the study of obesity (9–13) and glucose homeostasis (14). Thus, having 2 PET tracers (<sup>18</sup>F-FDG and <sup>18</sup>F-F-DA) that can image different aspects of BAT physiology may be potentially useful in future in vivo quantitative studies on humans or animal models, as has been proposed by other investigators for <sup>18</sup>F-FDG imaging of adipose tissue (38).

## CONCLUSION

The fact that <sup>18</sup>F-F-DA PET sometimes shows uptake in BAT should be kept in mind when these studies are interpreted. The proportion of our patients showing BAT on <sup>18</sup>F-FDG PET/CT was higher than that previously reported (3,4), possibly because of the high incidence of patients with increased sympathetic stimuli and pheochromocytoma in our series. The localization of <sup>18</sup>F-F-DA and <sup>18</sup>F-FDG is related to 2 important processes in BAT, namely adrenergic innervations and glucose metabolism, and quantitative PET using both agents may be helpful in further understanding the physiology and regulation of brown fat.

## ACKNOWLEDGMENTS

We acknowledge the support of the technologist and radiochemistry staff of the nuclear medicine and PET departments of Warren Grant Magnusson Clinical Center, NIH. The NIH Intramural Program provided financial support.

## REFERENCES

1. Hany TF, Gharehpapagh E, Kamel EM, Buck A, Himms-Hagen J, von Schulthess GK. Brown adipose tissue: a factor to consider in symmetrical tracer

- uptake in the neck and upper chest region. *Eur J Nucl Med Mol Imaging*. 2002;29:1393–1398.
2. Truong MT, Erasmus JJ, Munden RF, et al. Focal FDG uptake in mediastinal brown fat mimicking malignancy: a potential pitfall resolved on PET/CT. *AJR*. 2004;183:1127–1132.
  3. Cohade C, Osman M, Pannu HK, Wahl RL. Uptake in supraclavicular area fat (“USA-Fat”): description on <sup>18</sup>F-FDG PET/CT. *J Nucl Med*. 2003;44:170–176.
  4. Yeung HW, Grewal RK, Gonen M, Schoder H, Larson SM. Patterns of <sup>18</sup>F-FDG uptake in adipose tissue and muscle: a potential source of false-positives for PET. *J Nucl Med*. 2003;44:1789–1796.
  5. Fukuchi K, Ono Y, Nakahata Y, Okada Y, Hayashida K, Ishida Y. Visualization of interscapular brown adipose tissue using <sup>99m</sup>Tc-tetrofosmin in pediatric patients. *J Nucl Med*. 2003;44:1582–1585.
  6. Okuyama C, Sakane N, Yoshida T, et al. <sup>123</sup>I- or <sup>125</sup>I-metaiodobenzylguanidine visualization of brown adipose tissue. *J Nucl Med*. 2002;43:1234–1240.
  7. Okuyama C, Ushijima Y, Kubota T, et al. <sup>123</sup>I-Metaiodobenzylguanidine uptake in the nape of the neck of children: likely visualization of brown adipose tissue. *J Nucl Med*. 2003;44:1421–1425.
  8. Cannon B, Nedergaard J. Brown adipose tissue: function and physiological significance. *Physiol Rev*. 2004;84:277–359.
  9. Inokuma K, Okamatsu-Ogura Y, Omachi A, et al. Indispensable role of mitochondrial UCP1 for antiobesity effect of beta3-adrenergic stimulation. *Am J Physiol Endocrinol Metab*. 2006;290:E1014–E1021.
  10. Arch JR, Ainsworth AT, Cawthorne MA, et al. Atypical beta-adrenoceptor on brown adipocytes as target for anti-obesity drugs. *Nature*. 1984;309:163–165.
  11. Arch JR, Ainsworth AT, Ellis RD, et al. Treatment of obesity with thermogenic beta-adrenoceptor agonists: studies on BRL 26830A in rodents. *Int J Obes*. 1984;8(suppl 1):1–11.
  12. Nedergaard J, Petrovic N, Lindgren EM, Jacobsson A, Cannon B. PPARgamma in the control of brown adipocyte differentiation. *Biochim Biophys Acta*. 2005;1740:293–304.
  13. Avram AS, Avram MM, James WD. Subcutaneous fat in normal and diseased states: 2. Anatomy and physiology of white and brown adipose tissue. *J Am Acad Dermatol*. 2005;53:671–683.
  14. Valverde AM, Benito M, Lorenzo M. The brown adipose cell: a model for understanding the molecular mechanisms of insulin resistance. *Acta Physiol Scand*. 2005;183:59–73.
  15. English JT, Patel SK, Flanagan MJ. Association of pheochromocytomas with brown fat tumors. *Radiology*. 1973;107:279–281.
  16. Ricquier D, Nechad M, Mory G. Ultrastructural and biochemical characterization of human brown adipose tissue in pheochromocytoma. *J Clin Endocrinol Metab*. 1982;54:803–807.
  17. Melicow MM. Hibernating fat and pheochromocytoma. *AMA Arch Pathol*. 1957;63:367–372.
  18. Lean ME, James WP, Jennings G, Trayhurn P. Brown adipose tissue in patients with pheochromocytoma. *Int J Obes*. 1986;10:219–227.
  19. Goldstein DS, Chang PC, Eisenhofer G, et al. Positron emission tomographic imaging of cardiac sympathetic innervation and function. *Circulation*. 1990;81:1606–1621.
  20. Pacak K, Eisenhofer G, Carrasquillo JA, Chen CC, Li ST, Goldstein DS. 6-[<sup>18</sup>F]fluorodopamine positron emission tomographic (PET) scanning for diagnostic localization of pheochromocytoma. *Hypertension*. 2001;38:6–8.
  21. James W. *Research on Obesity*. London, U.K.: Her Majesty’s Stationery Office; 1976.
  22. Heaton JM. The distribution of brown adipose tissue in the human. *J Anat*. 1972;112:35–39.
  23. Cohade C, Mourtzikos KA, Wahl RL. “USA-Fat”: prevalence is related to ambient outdoor temperature—evaluation with <sup>18</sup>F-FDG PET/CT. *J Nucl Med*. 2003;44:1267–1270.
  24. Gelfand MJ. <sup>123</sup>I-MIBG uptake in the neck and shoulders of a neuroblastoma patient: damage to sympathetic innervation blocks uptake in brown adipose tissue. *Pediatr Radiol*. 2004;34:577–579.
  25. Tatsumi M, Engles JM, Ishimori T, Nicely O, Cohade C, Wahl RL. Intense (<sup>18</sup>F)-FDG uptake in brown fat can be reduced pharmacologically. *J Nucl Med*. 2004;45:1189–1193.
  26. Sundin U, Nechad M. Trophic response of rat brown fat by glucose feeding: involvement of sympathetic nervous system. *Am J Physiol*. 1983;244:C142–C149.
  27. Ramacciotti C, Schneegans O, Lang H, et al. Diffuse uptake of brown fat on computed-tomography coupled positron emission tomoscintigraphy (PET-CT) for the exploration of extra-adrenal pheochromocytoma [in French]. *Ann Endocrinol (Paris)*. 2006;67:14–19.
  28. Fukuchi K, Tatsumi M, Ishida Y, Oku N, Hatazawa J, Wahl RL. Radionuclide imaging metabolic activity of brown adipose tissue in a patient with pheochromocytoma. *Exp Clin Endocrinol Diabetes*. 2004;112:601–603.
  29. Goldstein DS, Coronado L, Kopin IJ. 6-[Fluorine-18]fluorodopamine pharmacokinetics and dosimetry in humans. *J Nucl Med*. 1994;35:964–973.
  30. Goldstein DS, Eisenhofer G, Dunn BB, et al. Positron emission tomographic imaging of cardiac sympathetic innervation using 6-[<sup>18</sup>F]fluorodopamine: initial findings in humans. *J Am Coll Cardiol*. 1993;22:1961–1971.
  31. Eisenhofer G, Hovey-Sion D, Kopin IJ, et al. Neuronal uptake and metabolism of 2- and 6-fluorodopamine: false neurotransmitters for positron emission tomographic imaging of sympathetically innervated tissues. *J Pharmacol Exp Ther*. 1989;248:419–427.
  32. Sturkenboom MG, Franssen EJ, Berkhof J, Hoekstra OS. Physiological uptake of [<sup>18</sup>F]fluorodeoxyglucose in the neck and upper chest region: are there predictive characteristics? *Nucl Med Commun*. 2004;25:1109–1111.
  33. Shimizu Y, Nikami H, Saito M. Sympathetic activation of glucose utilization in brown adipose tissue in rats. *J Biochem (Tokyo)*. 1991;110:688–692.
  34. Chernogubova E, Cannon B, Bengtsson T. Norepinephrine increases glucose transport in brown adipocytes via beta3-adrenoceptors through a cAMP, PKA, and PI3-kinase-dependent pathway stimulating conventional and novel PKCs. *Endocrinology*. 2004;145:269–280.
  35. Eldadah BA, Pacak K, Eisenhofer G, Holmes C, Kopin IJ, Goldstein DS. Cardiac uptake-1 inhibition by high circulating norepinephrine levels in patients with pheochromocytoma. *Hypertension*. 2004;43:1227–1232.
  36. Agostini D, Darlas Y, Filmont JE, et al. The reversibility of cardiac neuronal function after removal of a pheochromocytoma: an I-123 MIBG scintigraphic study. *Clin Nucl Med*. 1999;24:514–518.
  37. Garcia CA, Van Nostrand D, Atkins F, et al. Reduction of brown fat 2-deoxy-2-[<sup>18</sup>F]fluoro-D-glucose uptake by controlling environmental temperature prior to positron emission tomography scan. *Mol Imaging Biol*. 2006;8:24–29.
  38. Virtanen KA, Peltoniemi P, Marjamaki P, et al. Human adipose tissue glucose uptake determined using [<sup>18</sup>F]-fluoro-deoxy-glucose ([<sup>18</sup>F]FDG) and PET in combination with microdialysis. *Diabetologia*. 2001;44:2171–2179.